Commun. Optim. Theory 2024 (2024) 35 https://doi.org/10.23952/cot.2024.35

MATHRES Communications in Optimization Theory
Available online at http://cot.mathres.org

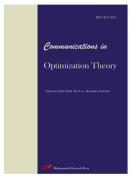

STABILITY AND PERFORMANCE ANALYSIS OF SYSTEMS WITH PARAMETER UNCERTAINTIES USING GENERALIZED D-DECOMPOSITION METHOD

ARIE NAKHMANI[1,*,†], HELEN BRINYARK[2,†], AVINASH SINGH[1], INCHAN J. YOON[3], RACHEL J. SMITH[1]

[1]Department of Electrical and Computer Engineering, University of Alabama at Birmingham, Birmingham, USA
[2]Department of Biomedical Engineering, University of Alabama at Birmingham, Birmingham, USA
[3]Department of Mechanical Engineering, University of Alabama at Birmingham, Birmingham, USA

Dedicated to Professor Ezra Zeheb on the occasion of his 85th birthday

Abstract. Stabilization of systems with multiple uncertain parameters is a challenging problem, but when particular performance characteristics are desired at the same time, the design problem becomes even more complex. In this work, we propose a novel way to achieve stability and performance of linear systems by generalizing the classical D-decomposition method. We propose designing continuous-time and discrete-time controllers for simultaneous stability and dynamic performance using the same methodology. The examples show its applicability to practical problems and provide relatively easy ways to extend the methodology to new kinds of uncertain systems.

Keywords. Controller design; D-decomposition; Generalized Nyquist theorem; Robust control; Stability.

2020 Mathematics Subject Classification. 93D09, 93B35.

1. INTRODUCTION

D-decomposition (or D-partition) is a classical mathematical technique used for stability analysis in the parameter space of linear systems proposed by Neimark [16, 17]. It also enables identifying a range of controller parameters that stabilize the system in the closed loop. The D-decomposition curves allow dividing the complex plane into sub-areas with a particular number of stable and unstable closed loop poles. The application of D-decomposition to a specific set of parameters has been found to facilitate analysis and provide valuable insights on stability, as discussed in [6, 18]. However, the application of D-decomposition becomes more difficult in systems of higher order. The utilization of the D-decomposition approach in higher order systems has several benefits, particularly in the domain of determining higher-order system parameters, such as the calculation of the global stability region. The global stability region for a given system can be successfully determined by employing

*Corresponding author. †Equal contribution.
E-mail address: anry@uab.edu (A. Nakhmani).
Received October 18, 2023; Accepted January 2, 2024.

the D-decomposition technique, as exemplified in [14]. The provided characterization provides significant insights into the stability of the system across a range of parameter values. Having a thorough understanding of the global stability domain is crucial for developing effective control strategies and improving system performance through careful optimization.

The various applications of D-decomposition cover a wide range of disciplines, including electrical system design and wind energy system design. D-decomposition technique is used to tune parameters of static VAR compensators to ensure their stability [7]. Ali et al. [1], present a robust multi-objective PID controller design using D-decomposition for an automatic voltage regulator and compare it to AI-based designs. Ayman and Soliman [3] propose using D-decomposition in the design of power system stabilizers. Optimizing PI voltage compensators for boost converters highlights the significance of D-decomposition [15], as it provides a systematic framework and facilitates Genetic Algorithm-based optimization. Dual Active Bridge converter regulation [10], robust current regulator design for grid-connected systems [21], and grid impedance variation mitigation [22] applications are using D-decomposition for a controller design. Moreover, D-decomposition methods ensure the stability and robustness of adaptive controllers for permanent magnet synchronous motor drives [8], as experimentally validated in comparison to conventional methods, or selecting controller parameters for a two-mass drive arrangement [9]. This D-decomposition method pinpoints the system's steady operational range. By reducing load speed overshoot and oscillations, classical and D-decomposition methods improve control. D-decomposition could also define wind energy conversion system (WECS) stability bounds [2]. Visualizing the D-decomposition technique displays excellent stability profile locations. These zones help the WECS damp oscillation, settling time, and overshooting analysis.

While the classical D-decomposition was defined for a single parameter design, a more recent body of work discusses multiple-parameter system stability and performance analysis. First, we will discuss the two-parameter system analysis. Pryashnikova [19] uses two real parameters to determine stability zones for polynomial equations with polynomially varying coefficients. D-decomposition domains approximate polynomial left half-plane zeros using rectangular patches. This approach may not work for higher-order parameters due to system constraints. This concept is extended to create robust stability domains in [20]. This study also introduces a new approach for computing the interval stability set for a two-parameter polynomial. Inscribed rectangles estimate the stability region, unlike the boundary-focused approach. This strategy seeks simple and effective ways to create stable parameter space regions [5]. Though it only works with low-dimensional parameters, this improves polynomial D-decomposition. The authors create root-invariant regions and stability domains. The work by Wang et al. [23] presents a new control strategy for continuous systems that may be subject to large uncertainties. The method concentrates on predicting output changes using estimation tools to deal with uncertainty more effectively than the prevalent adaptive extended state observer (ESO) method. It defines stability conditions and presents a D-decomposition method for determining stability-maintaining control ranges.

While a lot of progress has been made since the original introduction of the D-decomposition method, simultaneous stabilization and achievement of multi-parameter system's specifications remained challenging. Our work fills this knowledge gap and provides tools that allow both analysis of stability and performance and design of controllers.The novelty of the proposed method is in the ability to use it for discrete- and continuous-time systems with no change, to design almost arbitrary pole location regions that would satisfy both stability and performance specifications, and to find a

simple and easy to validate analytically and numerically set of inequalities that describe stabilizing subset of controllers that all also achieve desired specifications.

2. PRELIMINARIES

2.1. **D-decomposition for Characteristic Polynomials with one Parameter.** Given the characteristic polynomial in the continuous-time closed-loop system $D(s)$, let's assume that it depends on a single parameter K. For simplicity, we will assume that this parameter enters the characteristic polynomial linearly inside an arbitrary function f and there is part of this polynomial which depends on K and another part which does not:

$$D(s) = A(s) + f(K)B(s) = 0, \tag{2.1}$$

where $A(s)$ and $B(s)$ are some polynomials not dependent on K.

From Eq. (2.1) on the stability boundary $s = j\omega$, it follows that:

$$f(K) = -\frac{A(j\omega)}{B(j\omega)}; \quad -\infty < \omega < \infty. \tag{2.2}$$

If we plot the real part versus the imaginary part of $f(K)$, we get the D-decomposition curve in the parameter space of $f(K)$. The curve divides the complex plane into different sub-regions. Each sub-region should have specific number of stable roots. The reason is that for the number of stable roots to change, they must cross the $j\omega$ axis and be the root of $D(j\omega) = 0$ equation, but this is exactly how the D-decomposition curve was defined. In conclusion, if there is one region where for a particular $f(K)$ all roots are stable, then for the entire set of $f(K)$ in the same region the system is stable. To identify such a stability region, sometimes we need to test one K value in each segmented region, but we could do this also by looking for the inner-most region, as will be explained later.

Note that both stability and performance of a closed loop system are dependent on the location of its poles. It is possible to design such pole locations that the system will be stable and satisfy all performance requirements. Also, note that the stability boundary for the discrete-time systems is represented by the unit circle, so the desired location of poles for such systems will be inside the circle. Since plotting D-decomposition curves could be done on any arbitrary stability or performance boundary in the complex plane (instead of $j\omega$), we propose to parameterize and use these new regions for generalized D-decomposition.

2.2. **Generalized $\Gamma-$stability and Generalized Nyquist Curve.** In our previous work [11, 12, 13] we described a parametrization of a curve in the complex plane (see Figure 1) as:

$$\Gamma(\theta) = R(\theta)e^{j\theta} - \lambda, \tag{2.3}$$

where $\theta \in [0, 2\pi)$ is the angle parameter, λ is the real shift from the origin in the complex plane, and $R(\theta)$ is the radius-vector length for a particular angle θ.

While not all curves could be parameterized this way, most of the curves of interest for identifying regions of stability and performance could be written this way. For example, unit circle could be described by $\lambda = 0$ and $R(\theta) = 1$ for all θ. Given this parameterization, we were able to develop generalized Nyquist diagrams [11], define generalized $\Gamma-$stability (where all poles are located within the region outlined by Γ curve) and robust stability [12] and show how to design robust controllers that could $\Gamma-$stabilize the entire family of uncertain non-parametric systems [13]. Here we propose a parametric approach to system $\Gamma-$stabilization. The following section will describe our proposed methodology.

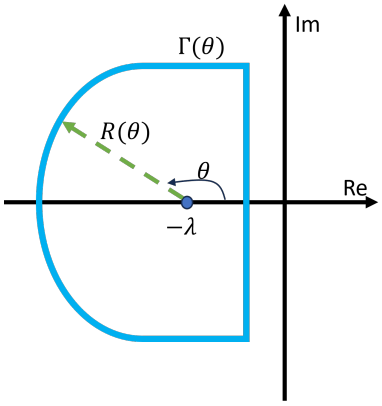

FIGURE 1. Parameterization of $\Gamma-$ stability region.

3. METHODS

3.1. **Uncertainty in a Single Parameter K.** Given the characteristic polynomial $D(s)$ of the system in a closed region, which includes an unknown parameter K, we define a curve $\Gamma(\theta)$ as before in the Eq. (2.3) and find for which values of K all the roots of $D(s)$ are within the region Γ. The development is done simply by applying the D-decomposition method by Neimark [16, 17] to the curve $\Gamma(\theta)$ instead of $j\omega$.
Let's assume that the characteristic equation can be written in the following form:

$$D(s;K) = A(s) + f(K)B(s) = 0; \quad deg(A(s)) > deg(B(s)), \tag{3.1}$$

where f is a certain function of K, $A(s)$, $B(s)$ - polynomials with constant coefficients.

Then the following holds:

$$f(K) = -\frac{A(s)}{B(s)}. \tag{3.2}$$

We construct the generalized Nyquist diagram [11] of the function $-A(s)/B(s)$ on the selected path $s = \Gamma(\theta) = R(\theta)e^{j\theta} - \lambda$, that is, we plot the real part of $f(K)$ versus the imaginary part of $f(K)$:

$$f(K) = -\frac{A(\Gamma(\theta))}{B(\Gamma(\theta))} = \mathrm{Re}\{-\frac{A}{B}(\theta)\} + j\,\mathrm{Im}\{-\frac{A}{B}(\theta)\}; \quad 0 \le \theta < 2\pi. \tag{3.3}$$

The resulting curve in the complex plane is a closed path and it divides the plane into several regions. Each region corresponds to a certain number of roots $D(s)$ has within the curve $\Gamma(\theta)$ (that we call region Γ for simplicity). The assignment of the value of $f(K)$ (which can also be a complex function of a complex variable K) into $D(s)$ at an arbitrary point within a certain region Γ, determines the number of zeros of $D(s)$ within Γ for all $f(K)$ obtained from any point within the same region. In case the number of zeros is equal to the order of the system, we obtain a $\Gamma-$stable system.

If we are dealing with real functions f and a real parameter K, we check the intersection points of the generalized Nyquist plot with the real axis, and between any two intersection points, we check one value of $f(K)$. If for this value the system is $\Gamma-$stable, then for all $f(K)$ in the aforementioned interval the system is $\Gamma-$stable.

Remarks:

(1) If the condition on the degree ratio of A and B is not satisfied, meaning the coefficients of the highest power in the characteristic polynomial depend on the parameter K, then we need to separate into 2 cases: the case where the coefficient of the highest power becomes zero (reducing the equation order) and the case where it does not become zero (normal case). Both cases will produce separate curves in the complex plane.
(2) If we find the possible range of variation for $f(K)$, we can also find the range of variation for K. In the case inverse function of f exists, $K = f^{-1}(f(K))$, but there is no need for invertibility requirement. We can find the range of variation for the parameter K from the image of $f(K)$.

Example 3.1. Given a transfer function in an open loop with a single parameter: $G(s) = (K^3 + 1)/(s^3 + K^3 s^2 + 20s + 4)$, we close the loop and obtain the characteristic polynomial in the closed loop: $D(s;K) = s^3 + K^3 s^2 + 20s + 4 + K^3 + 1 = s^3 + K^3 s^2 + 20s + 5 + K^3 = s^3 + 20s + 5 + K^3(s^2 + 1) = 0$.

From here: $K^3 = \frac{-s^3+20s+5}{s^2+1}$. We plotted the generalized Nyquist diagram for this function given $\Gamma(\theta) = 4e^{j\theta} - 5$ and obtained Figure 2.

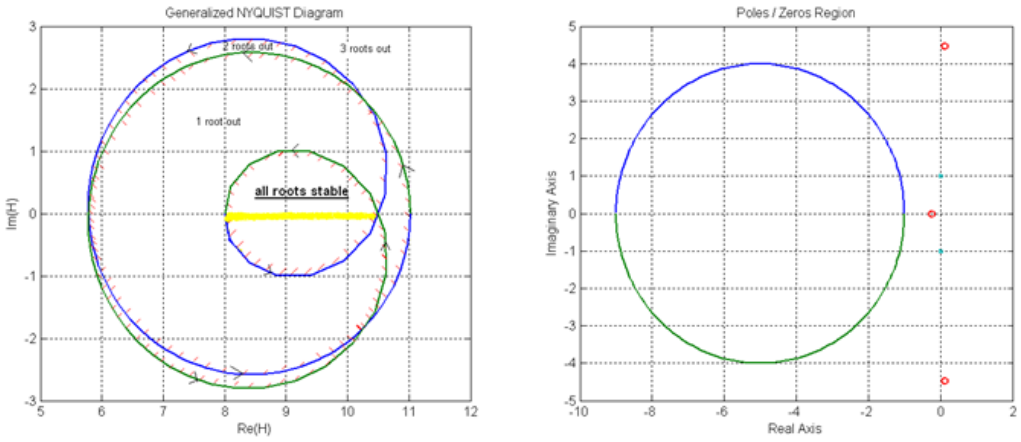

FIGURE 2. Finding the range of parameter K that gives a $\Gamma-$stable system.

From the graph on the left, it is clear that for all $8 < K^3 < 10.5$ the system is Γ-stable (as indicated in the diagram), and therefore the stability range of K is : $2 < K < \sqrt[3]{10.5}$. It can be observed that a similar approach can be used to find the stability range for a complex parameter K. In this case, the range is not only on the real axis but covers the entire $\Gamma-$stable region.

Note that if we move on the generalized Nyquist curve in the direction of increasing θ (denoted by the direction of arrows in Figure 2), and shade the left side of the curve, then each time we cross the curve from the shaded to non-shaded side, one root outside the Γ region is added. Given that the total number of roots is 3, and one needs to cross 3 lines (non-shaded to shaded) from outside to the innermost region, it is clear for the K values above all 3 roots are stable without verifying it for a particular value of K in this range.

3.2. **Uncertainty in Two Real Parameters K_1 and K_2.** Given the characteristic polynomial of the system in a closed loop $D(s;K_1,K_2)$ as a function of two unknown real parameters K_1 and K_2, we define a desired region $s = \Gamma(\theta) = R(\theta)e^{j\theta} - \lambda$ as we wish and find for which values of K_1 and K_2 all the roots of $D(s)$ lie within that region Γ. The desired region will be plotted in the parameter space of K_1 and K_2. For simplicity, let's assume that there is no reduction in the order of the characteristic

polynomial, meaning the coefficient of the highest power in the polynomial doesn't become zero for any parameter values.

We write down the characteristic equation:

$$D(s;K_1,K_2)_{s=\Gamma(\theta)} = f(\theta;K_1,K_2) = 0. \tag{3.4}$$

It is a complex equation that can be equated to its real and imaginary parts separately to obtain a system of two real equations. Let's assume there exists a solution to these equations in the following form:

$$\begin{cases} K_1 = f_1(\theta), \\ K_2 = f_2(\theta), \end{cases} \tag{3.5}$$

where f_1 and f_2 are real-valued, continuous, and defined for all $\theta \in [0, 2\pi)$, except for a finite number of points. In this case, we construct a parametric curve of f_2 as a function of f_1.

For points where f_1 or f_2 is not well-defined (usually when $\theta = 0$ or $\theta = \pi$), the solutions of Eq. (3.4) can be obtained as: $K_1 = f_3(K_2)$ (f_3 is a real-valued function). These functions are called special lines, and they represent solutions of the Eq. (3.4) for the corresponding frequency argument θ. These special lines are constructed in the same K_1 and K_2 plane and divide the parameter space into more sub-regions.

Let's examine a specific case where the parameters K_1 and K_2 appear linearly in the characteristic equation, i.e., $D(s;K_1,K_2) = K_1A(s) + K_2B(s) + C(s) = 0$, where A, B, and C are polynomials. We substitute $s = R(\theta)e^{j\theta} - \lambda$ into this equation and decompose A, B, and C into their real and imaginary parts. We obtain the following system of equations:

$$\begin{cases} K_1 \operatorname{Re}\{A(\theta)\} + K_2 \operatorname{Re}\{B(\theta)\} = -\operatorname{Re}\{C(\theta)\}, \\ K_1 \operatorname{Im}\{A(\theta)\} + K_2 \operatorname{Im}\{B(\theta)\} = -\operatorname{Im}\{C(\theta)\}. \end{cases} \tag{3.6}$$

According to Cramer's rule, the solution to the above linear system of equations is given by:

$$K_1(\theta) = \frac{\begin{vmatrix} -\operatorname{Re}\{C\} & \operatorname{Re}\{B\} \\ -\operatorname{Im}\{C\} & \operatorname{Im}\{B\} \end{vmatrix}}{\begin{vmatrix} \operatorname{Re}\{A\} & \operatorname{Re}\{B\} \\ \operatorname{Im}\{A\} & \operatorname{Im}\{B\} \end{vmatrix}} \quad K_2(\theta) = \frac{\begin{vmatrix} \operatorname{Re}\{A\} & -\operatorname{Re}\{C\} \\ \operatorname{Im}\{A\} & -\operatorname{Im}\{C\} \end{vmatrix}}{\begin{vmatrix} \operatorname{Re}\{A\} & \operatorname{Re}\{B\} \\ \operatorname{Im}\{A\} & \operatorname{Im}\{B\} \end{vmatrix}}. \tag{3.7}$$

For an argument that varies between 0 and 2π, we construct a parametric curve of $K_2(\theta)$ as a function of $K_1(\theta)$. Additionally, we construct special lines for the case when the numerator and denominator of Eq. (3.7) become zero. In this case, we go back to the system (3.6), substitute the corresponding argument, solve the system of equations again, and obtain a solution for K_1 and K_2.

Similar to the case with a single parameter, each parameter plane is divided into multiple regions by the parametric curves. It is sufficient to check one value of K_1 and K_2 in each region to determine the stability range. Alternatively, shading to the left side of the curves (while the argument θ is increased) could be applied similarly to Example 3.1.

Example 3.2. Given a transfer function in an open loop: $G(s) = 1/(s^2 + s + 1)$. We want to design a PD controller of the form $H(s) = K_1 s + K_2$ such that all poles in the closed loop system are located within a circle with a radius of 4 and shifted 5 units to the left from the origin.

Let's choose $\Gamma(\theta) = 4e^{j\theta} - 5$. We close the loop with unity feedback and obtain the characteristic polynomial in the closed loop $D(s;K_1,K_2) = s^2 + (K_1 + 1)s + K_2 + 1 = 0$. We substitute $\Gamma(\theta)$ and after basic trigonometric manipulations get:

$$f(\theta;K_1,K_2) = 16\cos(2\theta) - 36\cos(\theta) + 4\cos(\theta)K_1 + K_2 - 5K_1 + 21, \\ + j\,(16\sin(\theta) + 4\sin(\theta)K_1 - 36\sin(\theta))\,. \tag{3.8}$$

It follows that

$$\begin{aligned} &\mathrm{Re}\{A\} = 4\cos(\theta) - 5 && \mathrm{Im}\{A\} = 4\sin(\theta) \\ &\mathrm{Re}\{B\} = 1 && \mathrm{Im}\{B\} = 0 \\ &\mathrm{Re}\{C\} = 16\cos(2\theta) - 36\cos(\theta) + 21 \\ &\mathrm{Im}\{C\} = 16\sin(2\theta) - 36\sin(\theta). \end{aligned}$$

According to Eq. (3.7), $K_1 = 9 - 8cos(\theta)$; $K_2 = 40 - 40cos(\theta)$. Of course, we can write K_2 explicitly as a function of K_1 ($K_2 = 5(K_1 - 1)$), but it is not necessary. We plot this parametric curve (obtaining a single straight parametric line) in Figure 3.

We notice that the determinants become zero for $\theta = 0$ and $\theta = \pi$. In these cases, from Eq. (3.8), we obtain:

$$\theta = 0 \to 16 - 36 + 4K_1 + K_2 + 21 - 5K_1 = 0 \Rightarrow K_2 = K_1 - 1,$$
$$\theta = \pi \to 16 + 36 - 4K_1 + K_2 + 21 - 5K_1 = 0 \Rightarrow K_2 = -73 + 9K_1.$$

We construct the following two special lines in addition to the parametric line in the parameter space and obtain as shown in Figure 3.

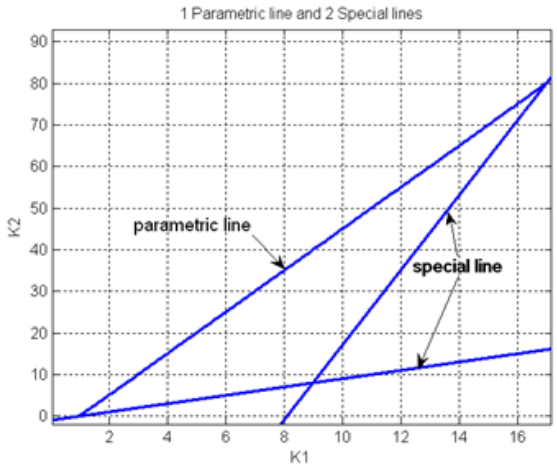

FIGURE 3. D-decomposition regions in K_1 and K_2 parameter space.

By directly testing one point [K_1,K_2] from each obtained region, we determine the Γ-stability region in Figure 4.

3.3. **Uncertainty in More Than Two Real Parameters.** When a system has more than two uncertain parameters, the D-decomposition method can also be used in a similar way. That is, similar to Eqs. (3.5) and (3.6), we equate a real and imaginary part to zero and obtain 2 equations with more than 2 unknowns:

$$\begin{cases} K_1\,\mathrm{Re}\{A_1(\theta)\} + \ldots + K_l\,\mathrm{Re}\{A_l(\theta)\} = -\mathrm{Re}\{C(\theta)\}, \\ K_1\,\mathrm{Im}\{A_1(\theta)\} + \ldots + K_l\,\mathrm{Im}\{A_l(\theta)\} = -\mathrm{Im}\{C(\theta)\}. \end{cases} \tag{3.9}$$

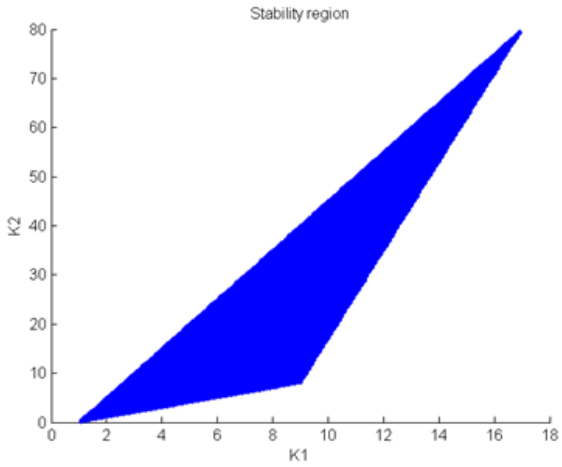

FIGURE 4. $\Gamma-$stability region in the K_1 and K_2 parameter space

In the case of more than 2 parameters, instead of lines separating the regions, we obtain $l-1$ dimensional hyperplanes (where l is the number of parameters). It is evident that visualizing such hyperplanes for more than 3 parameters is complicated. Real-world problems usually involve more than 2 parameters, so it is desirable to at least estimate the $\Gamma-$stability subregion in the parameter space. We propose a method to find an l-dimensional box within the $\Gamma-$stable parameter space. The center of this box is an arbitrary point in the $\Gamma-$stable parameter space, its edges are parallel to the coordinate system axes, and its volume is maximal. The discussion here is inspired by the work [4], but using $\Gamma-$stability instead of a regular stability.

Among the l parameters, we select two and without loss of generality denote them as K_1 and K_2. In this case, we can express the characteristic polynomial as:

(3.10)
$$D(s;K_1,...,K_l)|_{s=\Gamma(\theta)} = f(\theta;K_1,...,K_l) = K_1A(\theta;K_3,...,K_l)+K_2B(\theta;K_3,...,K_l)+C(\theta;K_3,...,K_l) = 0,$$

where A, B, and C are functions of the parameters and of θ.

Assuming that the point $\tilde{K}$ = ($\tilde{K}_1$, ..., $\tilde{K}_l$) in the parameter space yields a $\Gamma-$stable characteristic polynomial, i.e., all the roots of $f(\theta;\tilde{K}_1$, ..., $\tilde{K}_l)$ are within the region Γ. We assume that the point $\tilde{K}$ is calculated using other methods and is given to us. Then the volume of the box in the parameter space is given by:

$$V = 2^l(K_1-\tilde{K}_1)(K_2-\tilde{K}_2)\cdots(K_l-\tilde{K}_l), \tag{3.11}$$

where the edges have lengths: $2(K_i-\tilde{K}_i), i = 1,...,l$.

Similar to the case of 2 parameters, it is possible that the solution of Eq. 3.6 is given in the form of a parametric line:

$$\begin{aligned} K_1 &= K_1(\theta;K_3,...,K_l),\\ K_2 &= K_2(\theta;K_3,...,K_l). \end{aligned} \tag{3.12}$$

If there is also a special solution, it can be written as:

$$K_1 = K_1(K_2,...,K_l). \tag{3.13}$$

Substituting Eq. (3.12) into Eq. (3.11), we can maximize the volume by finding parameters for which:

$$\begin{aligned} &\frac{\partial V}{\partial \theta} = 0, \\ &\frac{\partial V}{\partial K_i} = 0, \quad i = 3,...,l. \end{aligned} \tag{3.14}$$

Substituting Eq. (3.13) into Eq. (3.11), we find the parameters which correspond to maximal volume by:

$$\frac{\partial V}{\partial K_i} = 0, \quad i = 2,...,l. \tag{3.15}$$

Let's assume that $\hat{K} = (\hat{K}_1,...,\hat{K}_l)$ is the solution that maximizes V and satisfies the constraints Eq. (3.12) and Eq. (3.14). Similarly, let's assume that $\bar{K} = (\bar{K}_1,...,\bar{K}_l)$ is the solution that maximizes V and satisfies the constraints Eqs. (3.13) and (3.15).

We define a set of boxes:

$$\{(K_1,...,K_l) \big| \big|K_i - \tilde{K}_i\big| \leq \min\{\big|\hat{K}_i - \tilde{K}_i\big|, \big|\bar{K}_i - \tilde{K}_i\big|\}, i = 1,...,l\}. \tag{3.16}$$

Assuming that the $\Gamma-$stability subregion is convex, it is evident that if every corner of this box is within this space. In the case of a non-convex space, we can find a convex sub-space that is contained within the given space. Euclidean norms can also be used [4] to solve non-convexity issues. Thus, using the set in Eq. (3.16), we can describe the l-dimensional box in a two-dimensional space.

Remarks:

(1) If the resulting box does not provide satisfactory results, i.e., the variation range for the number of parameters is not large enough, we can choose another point $\tilde{K}$ within the box and construct a new box around it, as before.

(2) There exist other methods for finding the stability radius for multi-parametric systems, e.g., using weighted p-norm [6]. These methods could be analytically developed only for limited classes of multi-parametric polynomials, while our method works for any polynomials. Also, the typical computation could require computing an intersection of polytopes in N-dimensional space, while our method provides a simple hyper-box within which all parameters provide $\Gamma-$stable system. For any p-norm-based stability radius, the stability hypersurface overlaps but does not coincide with the maximally possible hyper-box provided by our method. Thus, the hyper-box provides additional sub-regions of $\Gamma-$stabilizing parameter sets.

Example 3.3. Let's attempt to $\Gamma-$stabilize a transfer function $G(s) = 1/(s^2+s+1)$ with a PID controller $H(s) = 1/K_1 s + K_2 + K_3/s$, such that all poles in the closed-loop system are within a circle of radius 4 and shifted left from the origin by 5 units.

We choose $\Gamma(\theta) = 4e^{j\theta} - 5$, closing the unity feedback loop, and obtaining the characteristic polynomial in the closed loop $D(s;K_1,K_2,K_3) = s^3 + (K_1+1)s^2 + (K_2+1)s + K_3 = 0$. After substituting $s = \Gamma(\theta)$:

$$\begin{aligned} f(\theta;K_1,K_2,K_3) = &-105 + 25K_1 - 5K_2 + K3 + (264 - 40K_1 + 4K_2)\cos(\theta) + \\ &+ (16K_1 - 224)\cos(2\theta) + 64\cos(3\theta) + \\ &+ j4\sin(\theta)((8K_1 - 112)\cos(\theta) + 64\cos(\theta)^2 - 10K_1 + K_2 + 50). \end{aligned} \tag{3.17}$$

Therefore,

(3.18)
$$\begin{aligned}
&\mathrm{Re}\{A\} = 25 - 40\cos(\theta) + 16\cos(2\theta) && \mathrm{Im}\{A\} = 4\sin(\theta)(8\cos(\theta) - 10)\\
&\mathrm{Re}\{B\} = -5 + 4\cos(\theta) && \mathrm{Im}\{B\} = 4\sin(\theta)\\
&\mathrm{Re}\{C\} = -105 + K_3 + 264\cos(\theta) - 224\cos(2\theta) + 64\cos(3\theta)\\
&\mathrm{Im}\{C\} = 4\sin(\theta)(-112\cos(\theta) + 64\cos(\theta)^2 + 50)
\end{aligned}$$

and according to Eq. (3.7):

(3.19)
$$K_1(\theta, K_3) = \frac{\begin{vmatrix} -\mathrm{Re}C & \mathrm{Re}B \\ -\mathrm{Im}C & \mathrm{Im}B \end{vmatrix}}{\begin{vmatrix} \mathrm{Re}A & \mathrm{Re}B \\ \mathrm{Im}A & \mathrm{Im}B \end{vmatrix}} = \frac{-344\sin(2\theta) + 80\sin(3\theta) + (449 + K_3)\sin(\theta)}{41\sin(\theta) - 20\sin(2\theta)}$$

$$K_2(\theta, K_3) = \frac{\begin{vmatrix} \mathrm{Re}A & -\mathrm{Re}C \\ \mathrm{Im}A & -\mathrm{Im}C \end{vmatrix}}{\begin{vmatrix} \mathrm{Re}A & \mathrm{Re}B \\ \mathrm{Im}A & \mathrm{Im}B \end{vmatrix}} = \frac{(2040 + 10K_3)\sin(\theta) - (1640 + 4K_3)\sin(2\theta) + 400\sin(3\theta)}{41\sin(\theta) - 20\sin(2\theta)}.$$

There are also two special curves obtained when the lower determinant vanishes, that is, for $\theta = 0$ and $\theta = \pi$. Substituting these into Eq. (3.17) yields:

(3.20)
$$\begin{aligned}
K_1 &= K_2 - K_3 + 1,\\
K_1 &= \frac{1}{81}(657 + 9K_2 - K_3).
\end{aligned}$$

Now, choose an example Γ-stable point in the parameter space $\tilde{K} = (\tilde{K}_1, \tilde{K}_2, \tilde{K}_3) = (9.25, 33.3, 37)$. It is easy to verify that the roots of the polynomial $D(s) = s^3 + (\tilde{K}_1 + 1)s^2 + (\tilde{K}_2 + 1)s + \tilde{K}_3 = 0$ ($s_1 = -2.36$; $s_{2,3} = -3.95 \pm 0.34j$) are indeed within the circle $\Gamma(\theta) = 4e^{j\theta} - 5$. We construct the parametric curve and two special curves for $K_3 = \tilde{K}_3 = 37$ and obtain Figure 5.

Now, let's calculate the box with the maximum enclosed volume that includes $\Gamma-$stable parameters. The solution of Eq. (3.15) for the special curves gives a maximum point (calculated by a computer) for the first curve:

(3.21)
$$K_1 = K_2 - K_3 + 1 \Rightarrow \bar{K} = (5.26, 37.28, \mathbf{33.017})$$

and for the second special curve:

(3.22)
$$K_1 = \frac{1}{81}(657 + 9K_2 - K_3) \Rightarrow \bar{K} = (\mathbf{9.95}, 26.98, 93.82).$$

For the parametric curve, we solve the system of equations (3.14) and obtain potential extreme volume points:

(3.23)
$$\begin{aligned}
\hat{K} &= (8.44, 37.38, 1.63),\\
\hat{K} &= (8.53, 41.99, 72.11),\\
\hat{K} &= (7.14, 27.37, 47.02),\\
\hat{K} &= (11.25, \mathbf{30.46}, 47.28).
\end{aligned}$$

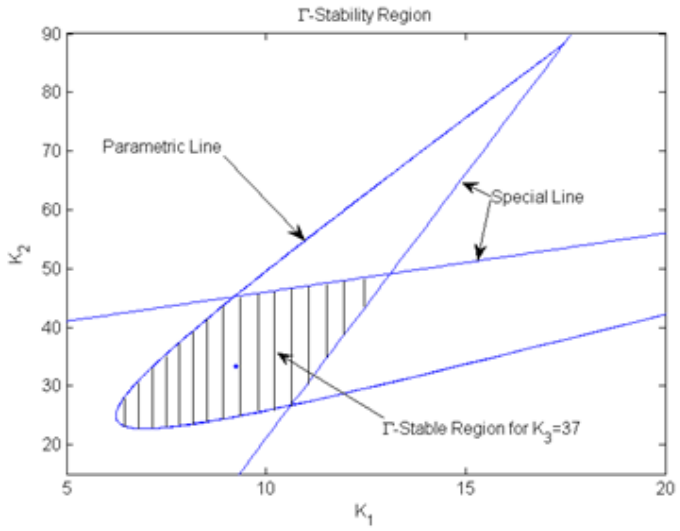

FIGURE 5. D-decomposition for Many Parameters

We need to find a box that is contained within all the boxes describing the extreme cases of maximum volume. Therefore, we choose their intersection, meaning we select the coordinates K_i closest to, $\tilde{K}_i$, as written in Eq. (3.16). Given $\tilde{K} = (9.25, 33.3, 37)$, we obtain a box (the closest points are highlighted in bold in the solution above):

$$
\begin{aligned}
&\left|K_1 - \underbrace{9.25}_{\tilde{K}_1}\right| \underset{\substack{\uparrow \\ K_1 close=9.95}}{<} 0.7 (= 9.95 - 9.25), \\
&\left|K_2 - \underbrace{33.3}_{\tilde{K}_2}\right| \underset{\substack{\uparrow \\ K_2 close=30.46}}{<} 2.84 (= 33.3 - 30.46), \\
&\left|K_3 - \underbrace{37}_{\tilde{K}_3}\right| \underset{\substack{\uparrow \\ K_3 close=33.02}}{<} 3.98 (= 37 - 33.02).
\end{aligned} \tag{3.24}
$$

We obtained a range of parameter values for which the system is $\Gamma-$stable in a closed loop. As can be seen, the solution does not require explicit construction of the curves and allows for expansion without changes for any number of parameters.

Remarks:

(1) The proposed method also works with non-affine and non-linear parameters.
(2) This method could be applied to discrete-time systems by using complex variable z instead of s and choosing appropriate Γ region of interest.
(3) While the provided examples could be computed manually, the computation and construction of the curves in the case of $\Gamma-$stability are complex, so they are performed typically using a computer. Even in finding the box, there is computational difficulty that does not allow for manual calculation, even for simple cases like a circle.

(4) In principle, the D-decomposition method does not assume that D(s) must be a polynomial. The method works without modifications for non-polynomial functions as well, such as exponential functions or systems with delays.

4. Conclusion

In this work, we proposed a novel methodology for analysis and design for systems with multiple parameters. We can rely on the extension of the D-decomposition method described in this work to examine the possible range for parameter variations in the system (in the parameter space), where all system poles remain within the predefined Γ region. Our approach allows simultaneous handling of stability and achieving desired performance specifications. The same methodology applies both to continuous- and discrete-time systems. We plan to extend it to other types of parametric and non-parametric uncertainties in our future work.

Acknowledgements
Research reported in this paper was supported in part by American Epilepsy Society Junior Investigator Award 1042632, CURE Epilepsy Foundation Taking Flight Award 1061181, and the UAB Consortium for Neuroengineering and Brain-Computer Interfaces Award. Arie Nakhmani expresses sincere gratitude to Dr. Ezra Zeheb for mentoring and guiding his research in control systems.

References

[1] M.N. Ali, M. Soliman, K. Mahmoud, J.M. Guerrero, M. Lehtonen, M.M.F. Darwish, Resilient design of robust multi-objectives PID controllers for automatic voltage pegulators: D-decomposition approach, IEEE Access 9 (2021) 106589-106605.

[2] M.N. Ali, M. Soliman, M.A. Ebrahim, M. Elsisi, D-decomposition-based multi-objective robust resilient control for blade pitch of wind energy conversion system, International Journal of Electrical Power and Energy Systems 146 (2023) 108781.

[3] M. Ayman, M. Soliman, Decentralised design Of robust multi-objective PSSs: D-decomposition approach, IET Generation, Transmission and Amp; Distribution 23 (2020) 5392-5406.

[4] J.H. George, On Parameter Stability Regions for Several Parameters Using Frequency Response, IEEE Transactions on Automatic Control 12 (1967) 197-200.

[5] E.N. Gryazina, B.T. Polyak, Stability regions in the parameter space: D-decomposition revisited, Automatica 42 (2006), 13-26.

[6] E.N. Gryazina, B.T. Polyak, and A. Tremba, D-decomposition technique state-of-the-art, Automation and Remote Control 69 (2008) 1991–2026.

[7] E. Jaramillo-Leon, R.R. Karymov, Application of the D-decomposition method using one parameter to select tuning parameters of static VAR compensators, 4th International Youth Conference on Radio Electronics, Electrical and Power Engineering (REEPE), pp. 1-6, 2022.

[8] H. Li, B. Song, T. Chen, Y. Xie, X. Zhou, Adaptive fuzzy PI controller for permanent magnet synchronous motor drive based on predictive functional control, Journal of the Franklin Institute 358 (2021) 7333-7364.

[9] K. Najdek, R. Nalepa and K. Szabat, Selection of controller parameters of a two-mass drive system using the D-decomposition technique, IECON 2019 - 45th Annual Conference of the IEEE Industrial Electronics Society, pp. 1308-1313, 2019.

[10] K. Najdek, R. Nalepa, The frequency- and the time-domain design of a dual active bridge converter output voltage regulator based on the D-decomposition technique, IEEE Access 9 (2021) 71388-71405.

[11] A. Nakhmani, M. Lichtsinder, E. Zeheb, Generalized Nyquist criterion and generalized bode diagram for analysis and synthesis of uncertain control systems, 24th IEEE Convention of Electrical and Electronics Engineers, pp. 250-254, 2006.

[12] A. Nakhmani, M. Lichtsinder, E. Zeheb, Generalized bode envelopes and generalized Nyquist theorem for analysis of uncertain systems, International Journal of Robust and Nonlinear Control 21 (2011) 752–767.
[13] A. Nakhmani, E. Zeheb, M. Lichtsinder, Robust controller design based on generalized bode envelopes, IMA Journal of Mathematical Control and Information 29 (201) 171-198.
[14] R. Nalepa, K. Najdek, K. Wrobel, K. Szabat, Application of D-decomposition technique to selection of controller parameters for a two-mass drive system, Energies 13 (2020) 6614.
[15] R. Nalepa, K. Najdek, B. Strong, Hybrid tuning of a boost converter PI voltage compensator by means of the genetic algorithm and the D-decomposition, Energies 14 (2021) 173.
[16] Yu.I. Neimark, On the distribution of roots of polynomials, Dokl. AN SSSR 58 (1947) 357–360.
[17] Yu.I. Neimark, On the structure of the D-decomposition of polynomials, Dokl. Akad. Nauk 1948.
[18] Y.P. Nikolaev, The geometry of D-decomposition of a two-dimensional plane of arbitrary coefficients of the characteristic polynomial of a discrete system, Automation and Remote Control 65 (2004) 1904-1914.
[19] P.F. Pryashnikova, D-decomposition in the case of polynomial dependence of the coefficients of a polynomial on two parameters, Autom. Remote Control 82 (2021) 398–409.
[20] P.F. Pryashnikova, Robust D-decomposition for a polynomial dependence of the coefficients of a polynomial on two parameters, Autom. Remote Control 83 (2022) 1078–1092.
[21] I. Tyuryukanov, M. Popov, D-decomposition based robust discrete-time current regulator for grid-connected VSI, IEEE 29th International Symposium on Industrial Electronics (ISIE), pp. 100-107, 2020.
[22] J. Wang, I. Tyuryukanov, A. Monti, Design of a novel robust current controller for grid-connected inverter against grid impedance variations, International Journal of Electrical Power and Energy Systems 110 (2019) 454-466.
[23] Q-G. Wang, T. Liu, Z-Y. Nie, S. Hao, X. Ren, D. Zhang, L. Wang, A generalized control scheme for system uncertainty estimation and cancellation, Transactions of the Institute of Measurement and Control, 43 (2021) 2921-2933.